

Novel Unimorph Adaptive Mirrors for Astronomy Applications

Peter Rausch, Sven Verpoort, and Ulrich Wittrock
Photonics Laboratory, Münster University of Applied Sciences
Stegerwaldstraße 39, 48565 Steinfurt, Germany.

rausch@fh-muenster.de, verpoort@fh-muenster.de, wittrock@fh-muenster.de

ABSTRACT

We have developed a new type of unimorph deformable mirror for the correction of low-order Zernike modes. The mirror features a clear aperture of 50 mm combined with large peak-to-valley amplitudes of up to 35 μm . Newly developed fabrication processes allow the use of prefabricated, coated, super-polished glass substrates. The mirror's unique features suggest the use in several astronomical applications like the compensation of atmospheric aberrations seen by laser beacons, low light astronomy, and the use in woofer-tweeter systems. Additionally, the design enables an efficient correction of the inevitable wave-front error imposed by the floppy structure of primary mirrors in future large space telescopes. We have modeled the mirror by using analytical as well as finite element models. We will present design, key features and manufacturing steps of the deformable mirror.

Keywords: unimorph deformable mirror, aberration compensation, adaptive optics, active optics

1. INTRODUCTION

Deformable mirrors are used to control the wave-front of coherent and incoherent light. Therefore these mirrors are tools of great importance in nearly all fields of optical sciences such as astronomy, ophthalmology, and laser physics. In astronomy for instance, wave-front errors severely limit the performance of telescopes. Terrestrial telescopes suffer from aberrations caused by atmospheric turbulences. While space telescopes avoid those atmospheric disturbances, their light-weighted primary mirrors may induce aberrations which vastly reduce the telescope performance [1].

In terrestrial telescopes, the use of deformable mirrors to overcome the atmospheric seeing limit is well established [2, 3], many types of deformable mirrors are commercially available [4, 5]. Our mirror distinguishes from many other mirror concepts by several features. The mirror laminate consists of a comparably thin glass substrate bonded onto a prefabricated PZT (lead zirconium titanate)-ceramic, which leads to a large stroke compared to other bimorph or unimorph mirrors. The glass substrate is polished and dielectrically coated before being bonded to the piezo disc. This procedure allows the use of highly reflective and extremely low scattering optical surfaces, which rival the best available passive optics. Furthermore, an integrated monolithic tip-tilt functionality allows alignment correction without the need for a separate tip-tilt mirror.

The design we present is being developed in the course of a project with the European Space Agency. The goal of this project is to design, manufacture, and test a space qualified adaptive deformable mirror. Such a mirror has never been employed in space telescopes so far. Space environment poses certain challenges to the mirror design in terms of heat management, mechanical stability, and operation in cryogenic vacuum environment. To meet these requirements, a strict selection of materials along with the development of an adequate mechanical design is necessary. Design and material parameters are described in section 2.

The mirror should enable wave-front correction in future large space telescopes, which suffer from wave-front imperfections due to the floppy structure of the primary mirror. The mirror should also be capable to be used with high power lasers. Powerful laser systems have become an important part in Earth observations missions, e.g. the laser of the ALADIN for the ADM-Aeolus mission. One challenge is to maintain a good beam quality during the amplification process(es) in such high-power systems. Here, an appropriately designed deformable mirror would help to improve the beam quality by compensating the detrimental aberrations.

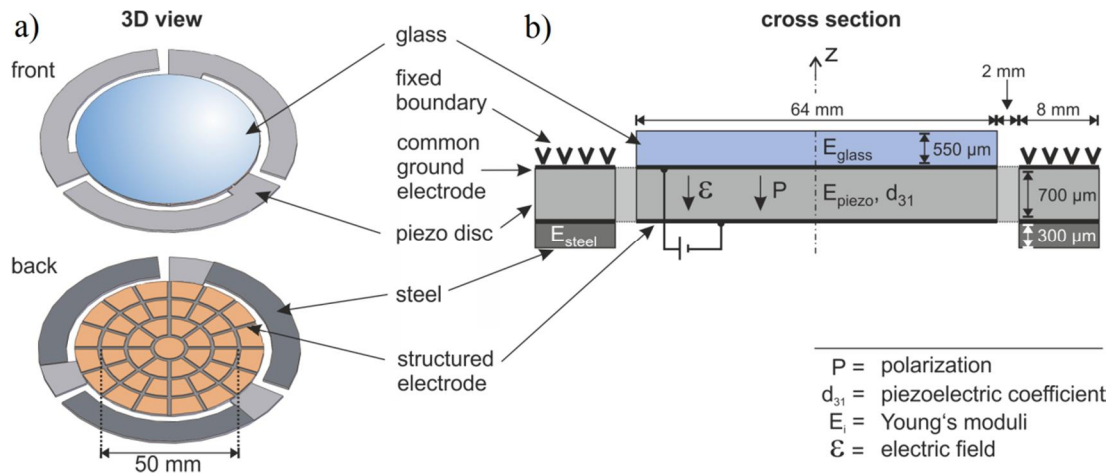


Fig. 1 a) Three-dimensional view of the deformable mirror along with the electrode pattern
 b) Cross-sectional view

2. MIRROR DESIGN

Figure 1 shows a three dimensional and a cross-sectional view of our mirror design. The mirror structure is based on a three-arm, laser-cut piezo disc which is sandwiched between two metallic electrodes. The unstructured front electrode serves as the common ground electrode while the structured backside electrode is used to actuate the mirror. Structuring of the electrode as well as cutting of the piezo disc is done by cold ps-laser ablation to avoid any heat-affected zone.

If a voltage is applied to the electrodes, the piezo disc strains azimuthally and radially due to the reverse piezoelectric effect. The strain is proportional to the piezoelectric coefficient d_{31} . The induced lateral stress between the piezo layer and the passive layer will cause a localized deformation of the laminate in the area of the actuated electrode.

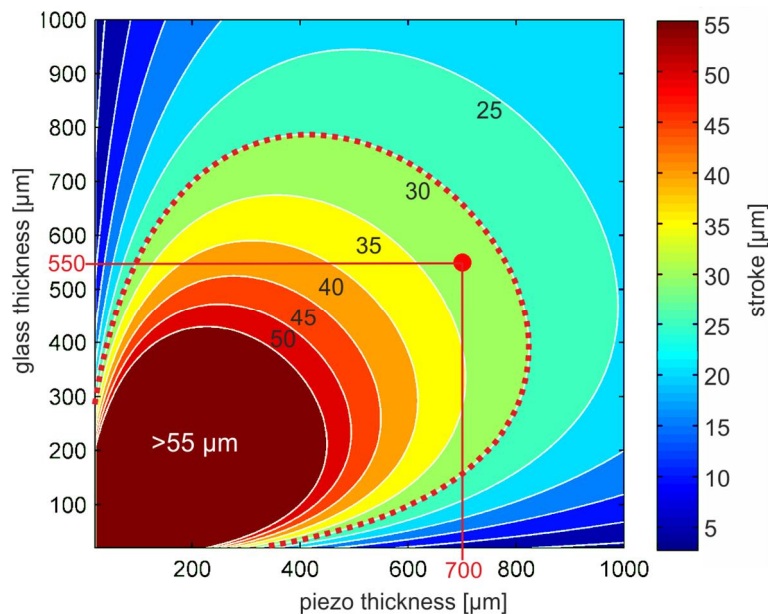


Fig. 2 Defocus stroke of the laminate as a function of individual layer thickness for an applied voltage of 400 V.

The back-side electrode is subdivided into a 40-electrode keystone pattern plus one center electrode (25 electrodes within the 50 mm optical aperture, 16 electrodes form an additional outer ring) and 3 electrodes to actuate the arms. This pattern has been found by analytical calculations and was optimized by means of finite-element calculations [6]. It enables a reproduction of low-order Zernike modes with high stroke and high fidelity.

A dielectrically coated, super-polished glass substrate is adhesively bonded to the front side of the piezo disc as passive layer. To meet the strict outgassing specifications as per ESA ECSS-Q-70, we use a low-outgassing UV-curable adhesive. Advantageous in terms of outgassing is the extremely small free surface of the adhesive layer. Outgassing only occurs around the circumference of the mirror structure where the resulting free surface is approximately 3 mm². To facilitate the tip-tilt functionality of the mirror, steel segments are adhesively bonded to the arms of the piezo structure and serve as a passive layer. To bond the segments onto the arms we use a heat-curing low outgassing epoxy.

Table 1. Geometry parameters and material specifications of the deformable mirror

Component	Property	Value
Piezo disc	Material:	PIC255 (Physik Instrumente)
	Disc thickness (μm):	700
	Total disc diameter (mm):	84
	Central disc diameter (mm):	64
	Optical aperture diameter (mm):	50
	Young's modulus (GPa):	62.9
	Coefficient of thermal expansion (10^{-6} K^{-1}):	4-8
Passive glass substrate	Piezoelectric coefficient d_{31} (10^{-12} mV^{-1}):	-174
	Material:	N-BK10
	Thickness (μm):	550
	Young's modulus (GPa):	72
Reflective coating	Coefficient of thermal expansion (10^{-6} K^{-1}):	5.88
	Type:	Dielectric Multilayer System
	Surface Roughness (\AA rms):	< 1.5
Adhesive layer	Reflectivity:	Arbitrary, e.g. BB-VIS
	Material:	Low-outgassing UV-curable adhesive
Passive steel segments	Thickness (μm):	~ 15
	Material:	Austenitic stainless steel
	Thickness (μm):	300
	Young's modulus (GPa):	200
Electrode Pattern	Coefficient of thermal expansion (10^{-6} K^{-1}):	10.8
	Number of actuators:	44
	Layout:	FEM optimized keystone pattern + 3 arm electrodes

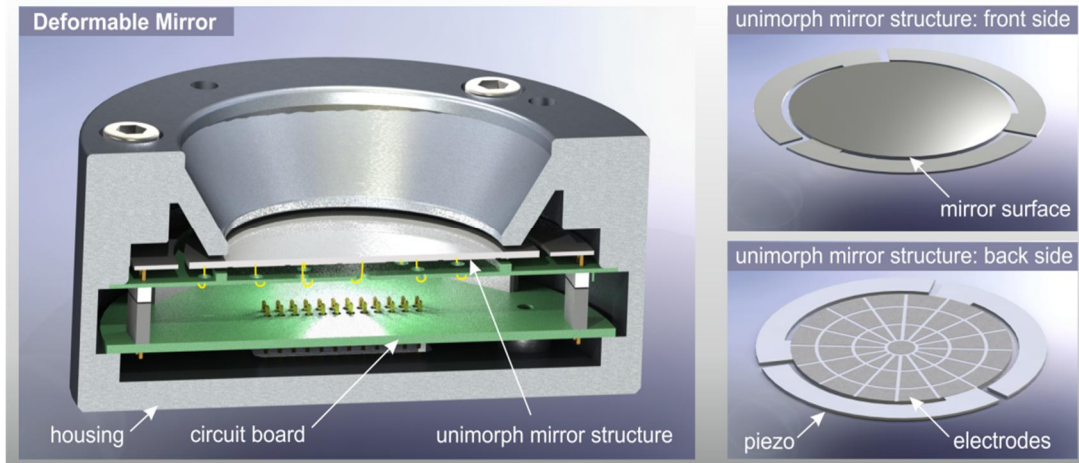


Fig. 3 Cross-sectional view of the assembled mirror (left) along with the laminate structure (right)

In a laminate consisting of two materials with different coefficients of thermal expansion (CTE), any changes of ambient temperature will cause the laminate to bend due to the bimetallic effect. During operation, the mirror could be exposed to environmental temperature changes. Therefore, mirror concepts are desirable which allow for matching the CTE's of the employed materials. Due to the simple design of the proposed mirror structure and the possibility to select the passive layers from a wide variety of materials, our mirror concept allows to match the CTE's. The manufacturer specifies the CTE of the employed piezo ceramic PIC255 with $4-8 \cdot 10^{-6} \text{ K}^{-1}$, the selected glass material N-BK10 exhibits a coefficient of $5.88 \cdot 10^{-6} \text{ K}^{-1}$. The CTE of piezo ceramics is not very well known and can differ significantly from batch to batch. We are currently measuring the low-temperature CTE of piezo ceramics to obtain a more precise value for the piezo materials we use.

Table 1 lists the geometry parameters and the material specifications of the deformable mirror. The thicknesses of the piezo layer and the glass layer have been optimized by means of analytical and numerical calculations. Figure 2 shows the achievable defocus stroke for piezo/glass laminates depending on the thickness of the individual layers at the maximum voltage of 400 V. This voltage is determined by the maximum applicable electric field strength of the piezo material. The red dot represents our selected thickness configuration. In our mirror design, the thicknesses of the laminate have been chosen to permit a defocus peak-to-valley deformation of $> 30 \mu\text{m}$. It can be seen that higher stroke could be achieved by using thinner piezo and glass discs. However, the stiffness of the laminate decreases with its thickness in the third power, leading to considerably more floppy structures, which is detrimental to the initial flatness. The selected thicknesses reflects a compromise between high stroke and sufficient initial flatness.

A cross sectional view of the mirror assembly is shown in figure 3 along with the unimorph laminate structure. The mechanical support of the mirror is designed to withstand vibrations and shocks which may be imposed on the assembly during the launch of the carrier vehicle.

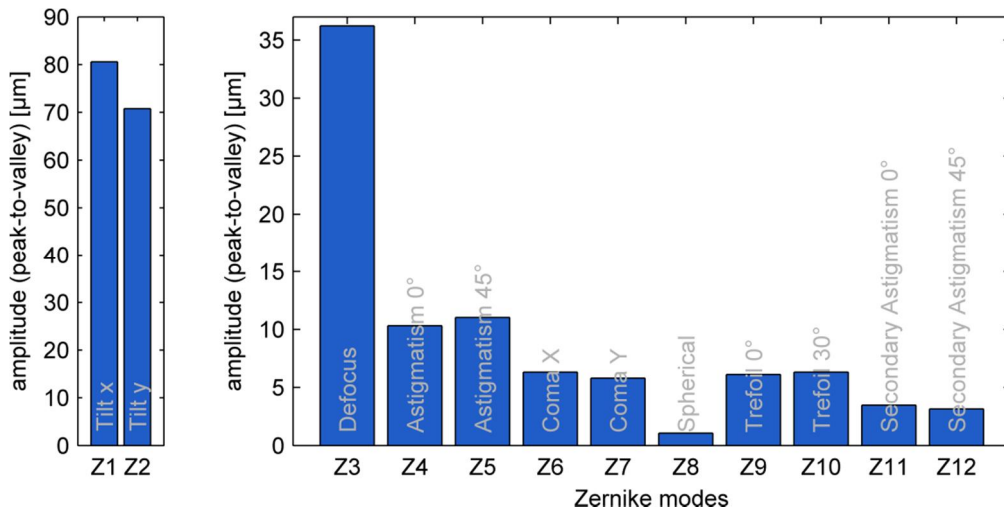


Fig. 4 Numerically calculated low order Zernike-amplitudes for the presented mirror configuration

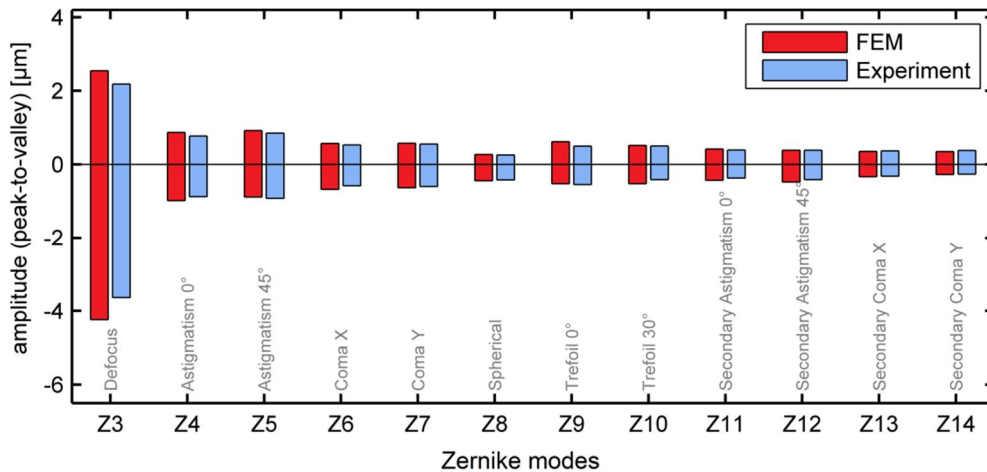


Fig. 5 Comparison between calculated and measured Zernike amplitudes generated by the smaller-sized prototype mirror

3. MIRROR CHARACTERIZATION

3.1 Generation of Zernike modes

The reproduction of Zernike modes up to the 12th order has been calculated via finite-element modeling and is shown in figure 4. The amplitudes are either limited by the maximum allowed voltage of 400 V, or if the residual wave-front error exceeds $\lambda/14$ (Maréchal-criterion) for $\lambda = 1064$ nm. Generally, the wave-front error increases with increasing amplitude, hence the latter criterion ensures diffraction-limited Zernike reproduction.

To validate the numerical model, a smaller-sized prototype mirror ($\varnothing 10$ mm) was fabricated and characterized. The measured and calculated Zernike amplitudes are shown in figure 5. The experimental results are in good agreement with the simulated values.

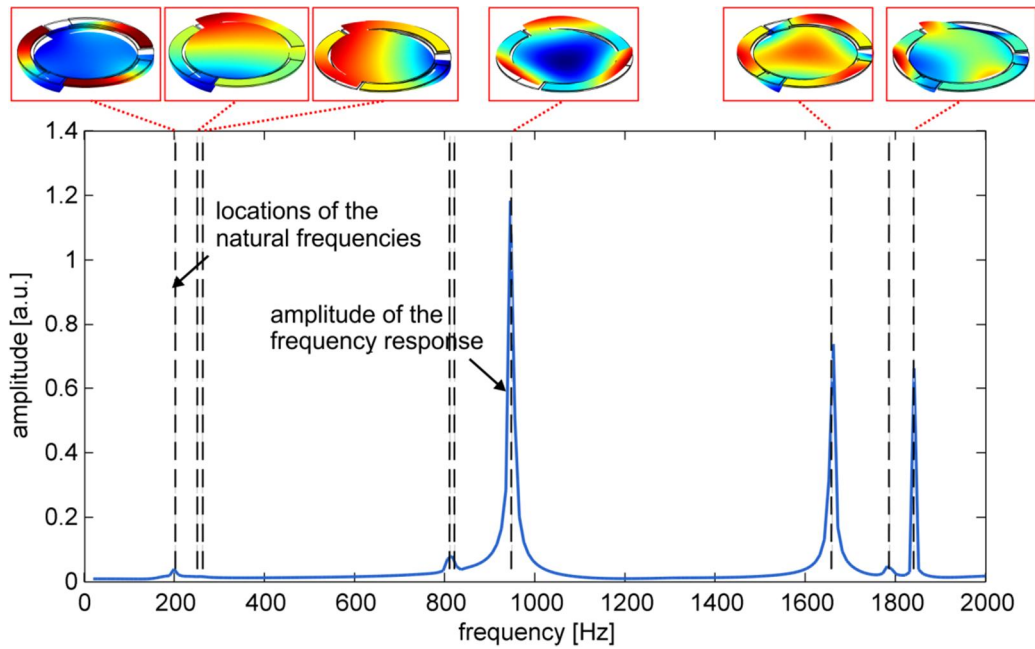


Fig. 6 Frequency response analysis of the first eigenfrequencies along with the corresponding eigenmodes

3.2 Dynamic Behavior

The behavior of the deformable mirror under dynamic actuation has been investigated by means of numerical calculations. Figure 6 shows the first eigenfrequencies along with the corresponding eigenmodes. The first eigenfrequencies occur at approximately 200 Hz.

The positions of the eigenfrequencies are directly related to the stiffness of the mirror structure. The eigenfrequencies can be shifted towards higher values by increasing the laminate stiffness. The first three eigenfrequencies are mainly determined by the stiffness of the three spiral arms. Accordingly, by stiffening merely the arms we can adapt the mirror to achieve higher actuation frequencies without reducing the performance of the central disc. This would solely entail a reduction of the tip-tilt amplitude.

3.3 Laser power handling capability

Our deformable mirror was originally invented for the use in high-power lasers. It has been experimentally confirmed that it withstands at least 7700 W of incident irradiation (1 μm wavelength) corresponding to an intensity of 560 kW/cm^2 . The experimental setup is shown in figure 7. A smaller-sized mirror (clear aperture: 12.7 mm) with identical reflective coating was used in a V-shaped high-power thin disc laser resonator. During laser operation, no mirror deformation or significant rise in temperature was detected.

The high power handling capability enables the use of our mirror to control the wave-front of a Laser Guide Star (LGS) adaptive optics system. In these systems, high power lasers are used to generate bright artificial guide stars in the atmospheric sodium layer. Light from this artificial guide star is used to measure the wave-front aberrations caused by atmospheric turbulences in a cone next to the science object. By controlling the wave-front of the LGS-beam, one might improve the performance of such an LGS system.

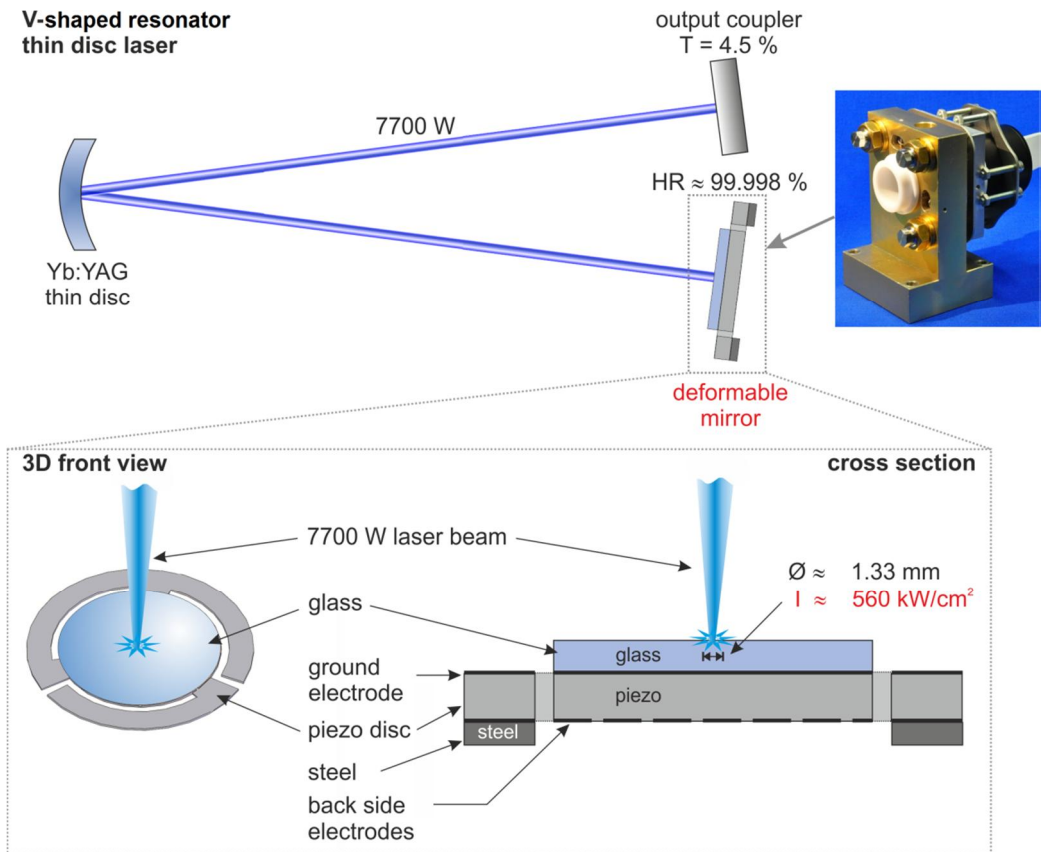


Fig. 7 Experimental setup to verify the power handling capability of the deformable mirror

4. CONCLUSION

We have presented a new concept for an adaptive deformable mirror. Its characteristics suggest the use in applications which require correction of low spatial frequency, large amplitude aberrations, and operation at medium temporal correction bandwidths. Applications could be the use as a woofer in a woofer-tweeter system or the correction of non-perfect large telescope optics. The flexible concept allows to scale the mirror aperture within one order of magnitude. It is possible to render the mirror insensitive to thermal fluctuations by smart selection of materials for the passive layers. We have demonstrated that the mirror is able to withstand high power laser irradiance, which gives rise to use the mirror in combination with high power lasers.

5. ACKNOWLEDGEMENTS

The authors gratefully acknowledge support for the work presented by the European Space Agency under contract number 4000104030/10/NL/EM.

REFERENCES

- [1] Allen, L., Angel, J. R. P., Mongus, J. D., Rodney, G. A., Shannon, R. R., Spoelhof, C. P. , “The Hubble Space Telescope optical systems failure report” , NASA Report (NASA, Washington D. C., Nov. 1990)
- [2] Beckers, J. M. “Adaptive optics for astronomy - Principles, performance, and applications”, Annual review of Astronomy and Astrophysics. Vol. 31 (A94-12726 02-90), p. 13-62.
- [3] Hardy, J. W. “Adaptive Optics for Astronomical Telescopes”, Oxford University Press (1998)
- [4] Poyneer, L. A., Bauman, B., Cornelissen, S., Isaacs, J., Jones, S., Macintosh, B. A., Palmer, D. W. “The use of a high-order MEMS deformable mirror in the Gemini Planet Imager”, Proc. SPIE, 7931 (2011)
- [5] Kudryashov, A., Shmalhausen, V., “Semipassive bimorph flexible mirrors for atmospheric adaptive optics applications” Optical Engineering, Vol. 35, p. 3064-3072 (1996)
- [6] Verpoort, S. and Wittrock, U. “Actuator patterns for unimorph and bimorph deformable mirrors”, Applied Optics, Vol. 49, No. 31, G37-G46 (2010)